








A novel method for measuring absolute coronary blood flow and microvascular resistance in patients with ischaemic heart disease

Paul D. Morris ^{1,2,3,*†}, Rebecca Gosling^{1,2,3†}, Iwona Zwierzak^{1,3}, Holli Evans ¹, Louise Aubiniere-Robb ¹, Krzysztof Czechowicz ¹, Paul C. Evans^{1,3,4}, D. Rodney Hose^{1,3,5}, Patricia V. Lawford ^{1,3}, Andrew J. Narracott ^{1,3‡}, and Julian P. Gunn ^{1,2,3‡}

¹Mathematical Modelling in Medicine Group, Department of Infection, Immunity and Cardiovascular Disease, Medical School, University of Sheffield, Sheffield, UK; ²Department of Cardiology, Sheffield Teaching Hospitals NHS Foundation Trust, Sheffield, UK; ³Insigneo Institute for In Silico Medicine, University of Sheffield, Sheffield, UK; ⁴The Bateson Centre, University of Sheffield, Sheffield, UK; and ⁵Department of Circulation and Medical Imaging, Norwegian University of Science and Technology (NTNU), Trondheim, Norway

Received 13 March 2020; revised 27 May 2020; editorial decision 7 July 2020; accepted 7 July 2020; online publish-ahead-of-print 14 July 2020

Aims

Ischaemic heart disease is the reduction of myocardial blood flow, caused by epicardial and/or microvascular disease. Both are common and prognostically important conditions, with distinct guideline-indicated management. Fractional flow reserve (FFR) is the current gold-standard assessment of epicardial coronary disease but is only a surrogate of flow and only predicts percentage flow changes. It cannot assess absolute (volumetric) flow or microvascular disease. The aim of this study was to develop and validate a novel method that predicts absolute coronary blood flow and microvascular resistance (MVR) in the catheter laboratory.

Methods and results

A computational fluid dynamics (CFD) model was used to predict absolute coronary flow (Q_{CFD}) and coronary MVR using data from routine invasive angiography and pressure-wire assessment. Q_{CFD} was validated in an *in vitro* flow circuit which incorporated patient-specific, three-dimensional printed coronary arteries; and then *in vivo*, in patients with coronary disease. *In vitro*, Q_{CFD} agreed closely with the experimental flow over all flow rates [bias +2.08 mL/min; 95% confidence interval (error range) -4.7 to +8.8 mL/min; $R^2 = 0.999$, $P < 0.001$; variability coefficient <1%]. *In vivo*, Q_{CFD} and MVR were successfully computed in all 40 patients under baseline and hyperaemic conditions, from which coronary flow reserve (CFR) was also calculated. Q_{CFD} -derived CFR correlated closely with pressure-derived CFR ($R^2 = 0.92$, $P < 0.001$). This novel method was significantly more accurate than Doppler-wire-derived flow both *in vitro* (± 6.7 vs. ± 34 mL/min) and *in vivo* (± 0.9 vs. ± 24.4 mmHg).

Conclusions

Absolute coronary flow and MVR can be determined alongside FFR, in absolute units, during routine catheter laboratory assessment, without the need for additional catheters, wires or drug infusions. Using this novel method, epicardial and microvascular disease can be discriminated and quantified. This comprehensive coronary physiological assessment may enable a new level of patient stratification and management.

[†]These authors are joint first authors.

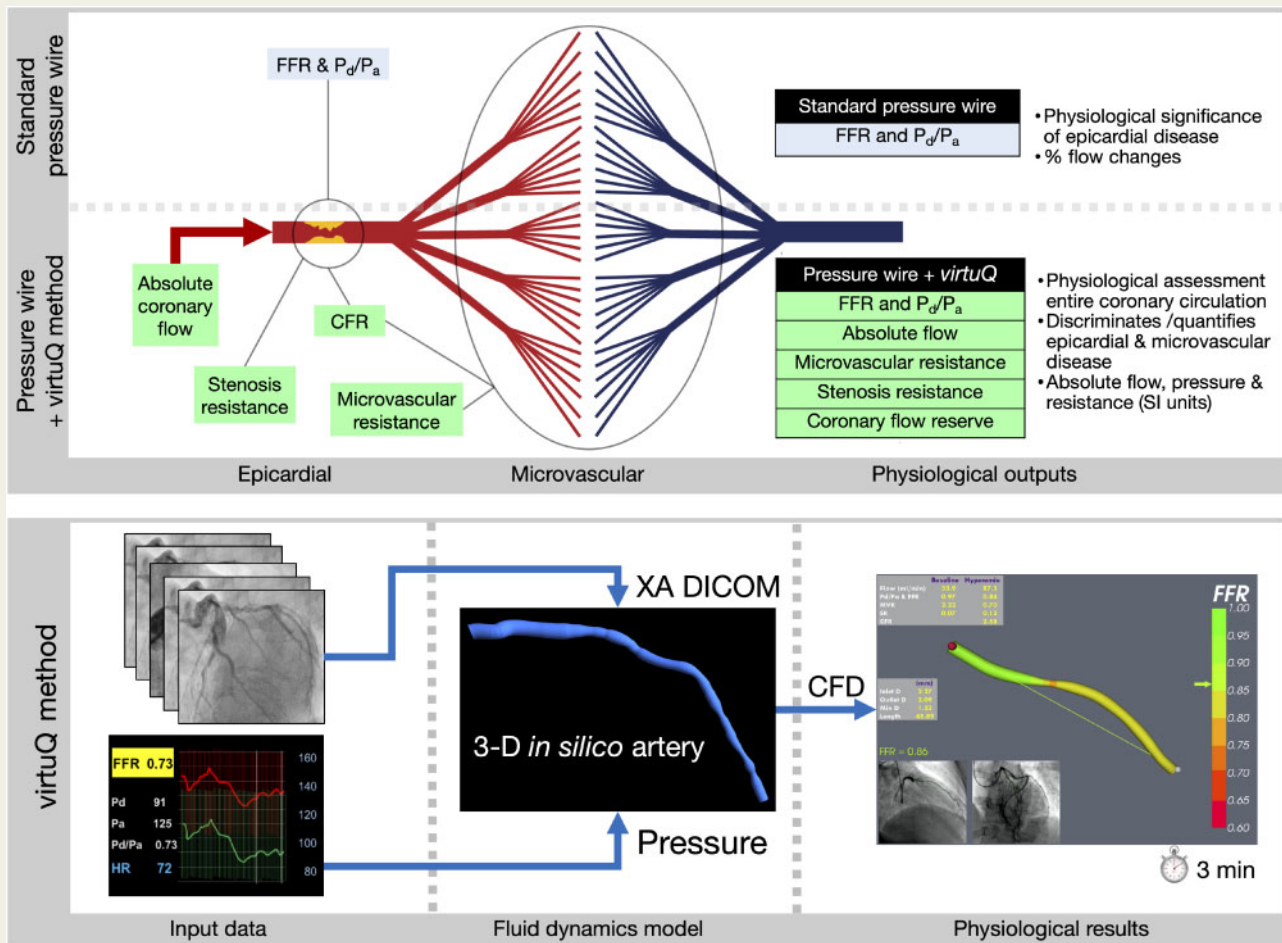
[‡]These authors are joint senior authors.

*Corresponding author. Tel: +44 (0) 114 215 9548; fax: +44 (0) 114 271 1863, E-mail: paul.morris@sheffield.ac.uk

© The Author(s) 2020. Published by Oxford University Press on behalf of the European Society of Cardiology.

This is an Open Access article distributed under the terms of the Creative Commons Attribution License (<http://creativecommons.org/licenses/by/4.0/>), which permits unrestricted reuse, distribution, and reproduction in any medium, provided the original work is properly cited.

Graphical Abstract



Keywords

Coronary blood flow • Computational fluid dynamics • Coronary physiology • Coronary angiography • Coronary microvascular dysfunction

1. Introduction

Ischaemic heart disease is caused by restricted coronary blood flow. Thus, measurements of coronary blood flow would be helpful to guide clinical interventions in the catheter laboratory. Coronary flow however, is challenging to measure and there are no methods for measuring it in routine clinical use. Conversely, measurement of intracoronary pressure is simple, accurate, and reproducible. Consequently, cardiologists use translesional pressure measurements as a proxy for changes in blood flow. Examples include fractional flow reserve (FFR) and instantaneous wave-free ratio (iFR). These pressure-derived, surrogate flow indices are used widely to estimate the blood flow reduction due to epicardial coronary disease and guide the appropriateness of percutaneous coronary intervention (PCI). Use of FFR and iFR to guide PCI has become established in routine interventional practice and, compared with traditional angiography, has improved clinical outcomes.¹⁻³

Such is the popularity and efficacy of these pressure-derived indices, that it is perhaps easy to overlook some limitations. First, FFR and iFR

focus exclusively on the epicardial arteries and they cannot discriminate, or quantify microvascular disease. This is a significant limitation because coronary microvascular dysfunction (MVD) affects >50% of those assessed in the catheter laboratory, is prognostically important, is implicated in the 20% of patients with persistent angina after revascularization, affects women disproportionality, consumes excessive healthcare resources, and responds to European Society of Cardiology (ESC) guideline-indicated treatment.⁴⁻⁹ Yet, because it is overlooked by pressure-derived indices, MVD remains undiagnosed and untreated in many patients.⁹ Second, FFR and iFR predict a *percentage* flow restriction, but of an unknown value. They do not measure the actual (absolute) flow reduction in mL/min. Because relieving ischaemia is the main target for PCI,^{10,11} the ability to measure flow reduction in absolute terms may be beneficial. Unless absolute flow is measured, the true magnitude of the flow reduction cannot be known. Whilst there may be a broad correlation between FFR and absolute flow restriction, knowing whether an FFR of 0.80 represents a 20 or 120 mL/min reduction in coronary flow can only add value to the coronary physiological assessment.

If both pressure and flow could be measured reliably and simply, a number of additional physiological parameters could be calculated using basic haemodynamic laws. These include microvascular resistance (MVR), stenosis resistance (SR), and coronary flow reserve (CFR), all of which help to discriminate and independently assess microvascular and epicardial coronary disease, thus providing a comprehensive physiological assessment of the entire coronary circulation.

To enable this 'next-level' of coronary physiological assessment, there is therefore, a need for a method that measures absolute coronary blood flow, in combination with intracoronary pressure, practical for routine use in the cardiac catheter laboratory. The aim of this study was to develop and validate a novel computational fluid dynamics (CFD) based method which, with a standard pressure wire, could assess absolute coronary blood flow, and all relevant coronary physiological indices, including MVR.

2. Methods

This research was performed at the University of Sheffield and Sheffield Teaching Hospitals NHS Foundation Trust UK, conformed to the principles of the Declaration of Helsinki and was approved by the NHS Health Research Authority, Regional Ethics Committee. Participating patients provided informed consent.

2.1 The computational model

Model inputs were standard coronary angiographic (digital imaging and communications in medicine, DICOM) images and pressure data. The principal model output was absolute coronary flow (Q_{CFD}) in mL/min. Three-dimensional coronary anatomy was reconstructed within the virtuQ software from two, two-dimensional angiographic projections, acquired $\geq 30^\circ$ apart during end-diastole, producing an axisymmetric three-dimensional (3D) model.^{12,13} Volume mesh was constructed with 1.2–1.5 M elements. Pressure boundary conditions were applied at the inlet and outlet, informed by the invasively measured values.¹⁴ CFD simulation was performed (ANSYS, PA, USA) on a Dell Precision T5600 computer (Intel Xeon E5 2650, 2 GHz processor, 32GB RAM) to a residual target of 10^{-6} .¹² The arterial wall was considered rigid. The Q_{CFD} method is outlined in Figure 1. Using the hydraulic equivalent of Ohm's law, Q_{CFD} and pressure data were used to calculate coronary MVR, SR, and CFR under baseline (BL) and hyperaemic (Hyp) conditions as follows:

$$\begin{aligned} MVR &= \frac{P_d}{Q_{CFD}} \\ SR &= \frac{P_a - P_d}{Q_{CFD}} \\ CFR &= \frac{Q_{CFD}^{Hyp}}{Q_{CFD}^{BL}} \end{aligned}$$

2.2 In vitro assessment

Q_{CFD} accuracy was validated in an *in vitro* flow circuit outlined in Figure 2. To provide realistic experimental conditions, patient-specific coronary arteries were 3D printed. Cases included left anterior descending artery (LAD), right coronary artery (RCA), and left circumflex artery (LCX). Percentage diameter stenosis ranged from 46% to 72% and lengths ranged from 68 mm to 84 mm. Case-specific details of the individual models and of the 3D printing protocol can be found in the

Supplementary material online. Flow rates were varied from 50 to 180 mL/min in 10 mL/min increments. Assuming a baseline flow of 60 mL/min and a CFR of up to three (in the context of flow-limiting lesions), this reflects a broad physiological range from baseline through hyperaemic conditions.

Proximal pressure (P_a) was measured using a TruWave Pressure Transducer (Edwards Lifesciences Corp, USA) and distal pressure (P_d) with a Volcano Primewire (Philips Volcano, Philips Healthcare, Best, Netherlands). Experimental flow rate (Q_{Exp}) was repeatedly calibrated (prior to every analysis) by measuring the fluid volume draining into a flask in one minute. Coronary models were run at all 14 flow rates. Each was repeated three times, with a mean result recorded. Four-hundred and twenty analyses were performed in total. The pressure gradient ($P_a - P_d$) was applied as a pressure boundary condition at the inlet with zero pressure at the outlet. For Doppler analysis, an ultrafine nylon powder (Orgasol® Powders, Arkema Group, Colombes, France) was added to the blood-analogue fluid to mimic the ultrasonic back-scatter properties of erythrocytes.¹⁶ Doppler flow velocity was measured with a Philips Volcano Doppler FloWire® (Philips Volcano, CA, USA). The Doppler wire was positioned and manipulated until the optimal (most dense) Doppler signal was recorded. Coronary flow derived from Doppler ultrasound measurements (Q_{Dop}) was calculated from Doppler flow average peak velocity (APV), assuming a parabolic laminar flow profile ($APV = 2 \times$ mean velocity), by considering the luminal cross-sectional area ($V = Q/A$), where A was known precisely from the print files.

The primary outcome measure was the accuracy of computed flow rate, Q_{CFD} , compared with the calibrated Q_{Exp} . Physiological flows are typically laminar [Reynolds (Re) number < 500] but the experimental protocol had potential to induce supra-physiological flow rates (180 mL/min through severe stenosis).¹⁷ We therefore also report accuracy for the subset of cases where Reynolds number (Re) is less than 500 ($Re = \frac{\rho V D}{\mu}$ where V is the average velocity over the circular cross-section at the location with minimum diameter (stenosis), D the diameter at this location and ρ and μ the density and viscosity, respectively).

To investigate whether there was any additional value in terms of increased Q_{CFD} accuracy in simulating pulsatile flow we also ran all the models at all flow rates under both steady and pulsatile flow profiles and simulated likewise in the computational model. Mean P_a and P_d were applied for steady analysis, and transient P_a and P_d measurements (with transient analysis) for pulsatile. Details regarding how flow pulsatility was imposed in the flow circuit can be found in the Supplementary material online.

2.3 First-in-man *in vivo* assessment

Angiographic and invasive pressure data were collected from a previously unstudied cohort of 40 patients with stable coronary artery disease. Patients with history of coronary artery bypass surgery were excluded. Q_{CFD} was computed using the computational model as described above under baseline and hyperaemic conditions with time averaged P_a and P_d applied as the inlet and outlet boundary conditions, respectively measured simultaneously from the pressure wire and guide catheter. MVR, SR, and CFR were calculated using the equations above. An independent operator repeated 24 Q_{CFD} , MVR, and Q_{CFD} -derived CFR analyses to derive interobserver variability. A subset of 20 patients also underwent Doppler flow wire (FloWire®, Philips Volcano, NL) assessment, from which coronary flow (Q_{Dop}) and CFR ($Q_{Dop}^{Hyp}/Q_{Dop}^{BL}$) were derived. Measurements were repeated three times and the mean value was recorded. Pressure-derived CFR (CFR_{P-D}) was also calculated according to:

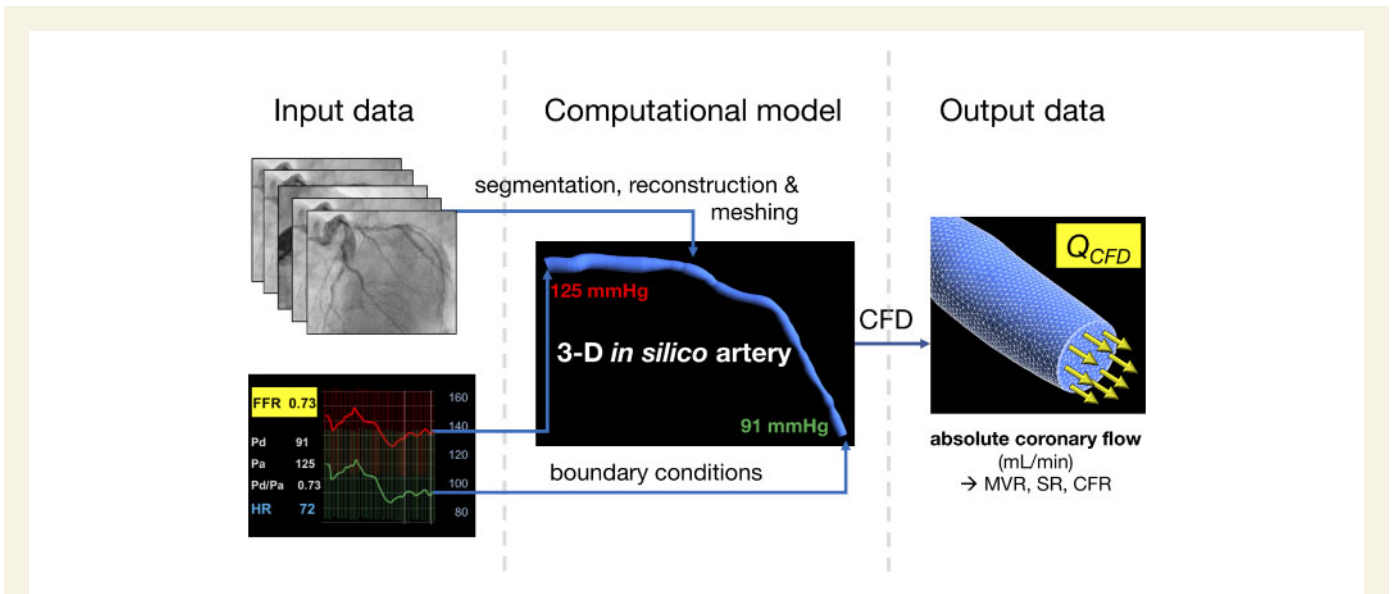


Figure 1 The computational method for computing absolute coronary blood flow. Coronary angiographic images are used to reconstruct the coronary anatomy. Pressure data are used to tune boundary conditions. CFD simulation computes the volumetric flow rate (Q_{CFD}), which enables coronary microvascular resistance (MVR), stenosis resistance (SR), and coronary flow reserve (CFR) to be calculated automatically.

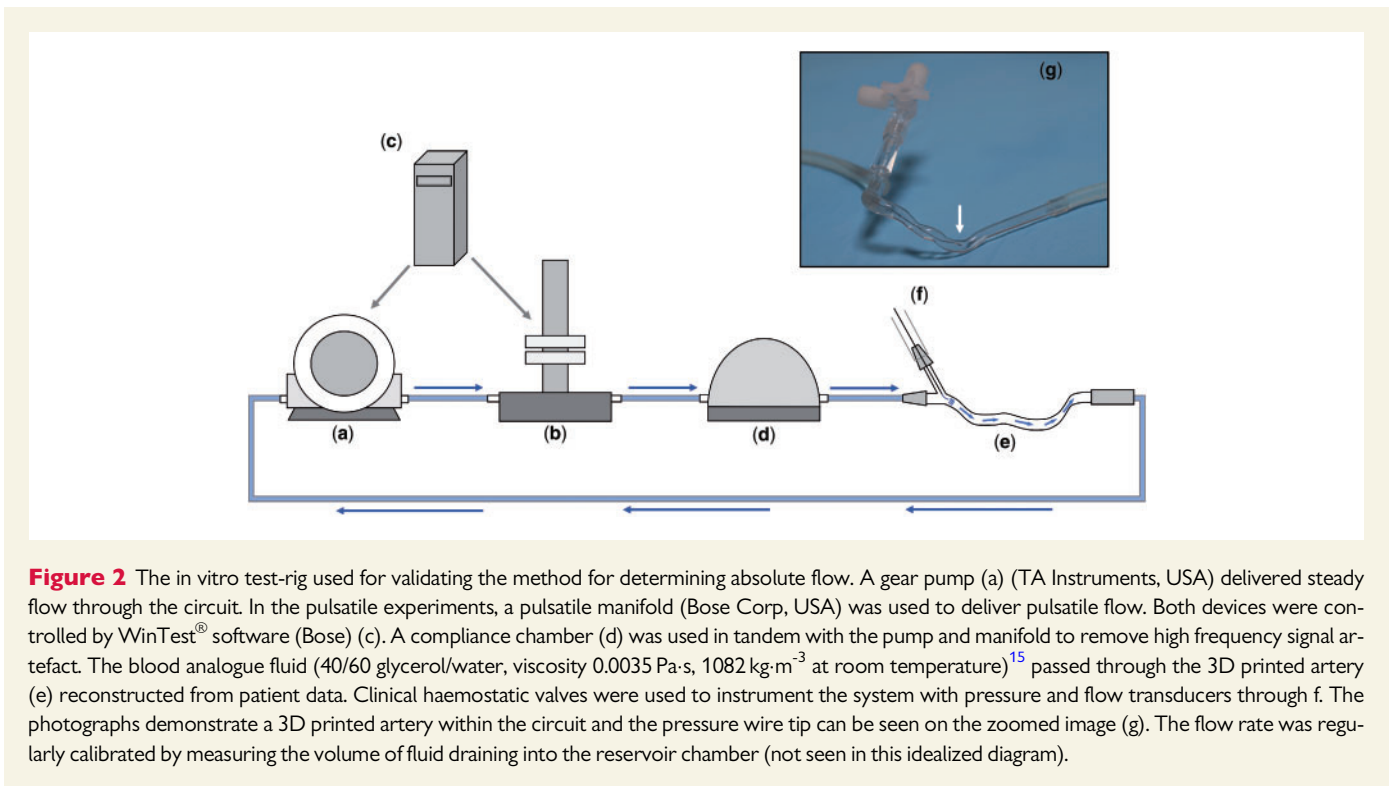


Figure 2 The in vitro test-rig used for validating the method for determining absolute flow. A gear pump (a) (TA Instruments, USA) delivered steady flow through the circuit. In the pulsatile experiments, a pulsatile manifold (Bose Corp, USA) was used to deliver pulsatile flow. Both devices were controlled by WinTest[®] software (Bose) (c). A compliance chamber (d) was used in tandem with the pump and manifold to remove high frequency signal artefact. The blood analogue fluid (40/60 glycerol/water, viscosity 0.0035 Pa·s, 1082 kg·m⁻³ at room temperature)¹⁵ passed through the 3D printed artery (e) reconstructed from patient data. Clinical haemostatic valves were used to instrument the system with pressure and flow transducers through f. The photographs demonstrate a 3D printed artery within the circuit and the pressure wire tip can be seen on the zoomed image (g). The flow rate was regularly calibrated by measuring the volume of fluid draining into the reservoir chamber (not seen in this idealized diagram).

$$CFR_{P-D} = \sqrt{P_a - P_d \text{ hyperaemic}} / \sqrt{P_a - P_d \text{ baseline}}$$

CFR_{P-D} is known to correlate closely with CFR.¹⁸ CFR_{P-D} was therefore compared with CFR derived from the novel Q_{CFD} method ($CFR_{Q_{CFD}}$) and that derived from Doppler (CFR_{Dop}). We also compared the pressure drop computed by the computational model with flow applied as the inlet boundary condition using both Q_{CFD} and Q_{Dop} .

2.4 Statistical analysis

Unless stated otherwise, mean delta and standard deviation (SD) of the mean are presented. Agreement was assessed using Bland–Altman plots. Bland–Altman limits of agreement (± 1.96 SD), which comprise 95% of all results, were used as the error range.¹⁹ Reproducibility was assessed by calculating the coefficient of variation (CoV) as the ratio of the

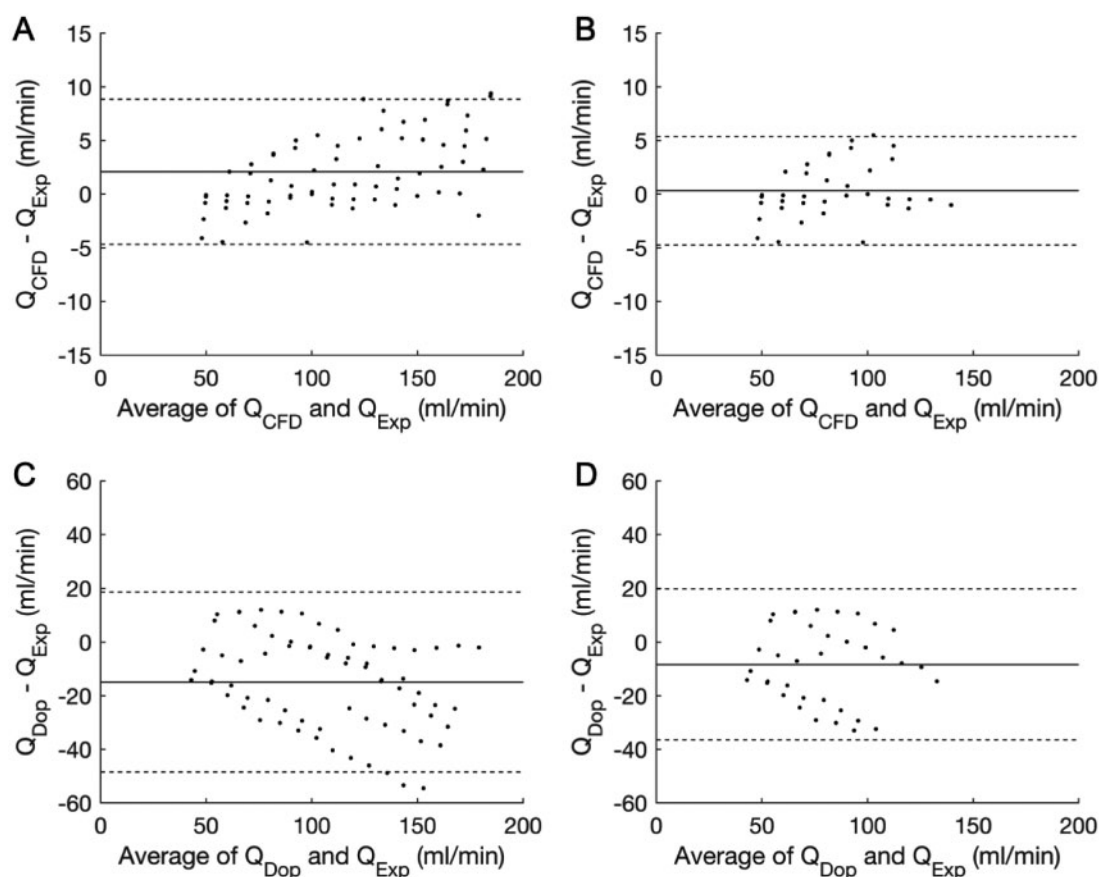


Figure 3 Bland–Altman plots demonstrating the accuracy of Q_{CFD} and Q_{Dop} . (A) The accuracy of the novel Q_{CFD} method over all flow rates [bias +2.08 mL/min; limits of agreement (± 1.96 SD) ± 6.75 mL/min]. (B) The accuracy of Q_{CFD} for cases with $Re \leq 500$ (bias +0.31 mL/min; limits of agreement ± 5.0 mL/min). (C) The accuracy of the Doppler method (Q_{Dop}) over all flow rates (bias -14.9 mL/min; limits of agreement ± 33.5 mL/min). (D) The accuracy of the Doppler method for cases with $Re \leq 500$ (bias -8.34 mL/min; limits of agreement ± 28.1 mL/min). The solid line indicates the bias (mean delta) and the broken lines indicate the limits of agreement (± 1.96 SD). Both methods were plotted against the gold-standard of the calibrated experimental flow rate (Q_{Exp}). Note the difference in Y-axis scale between the two methods. Each dot represents the average of three recordings, i.e. 70 data points and 210 samples.

standard deviation and mean values of repeated samples. Pearson coefficient (r) was used to calculate linear correlation and R^2 . Seventeen or more paired samples were required to detect $r \geq 0.70$ at 0.05 significance and 0.90 power. Analysis was performed using SPSS (IBM Corp, USA).

3. Results

3.1 Accuracy of steady CFD analysis

In all cases, over all flow rates, the difference between steady and pulsatile flow was negligible (bias -0.2 mmHg SD 0.9 mmHg equating to <1 mL/min difference). Given that steady CFD analysis, based on time-averaged pressure boundary conditions is considerably quicker and simpler to compute, we elected to use this model for the (*in vivo*) analysis. Further details of this analysis can be found in the [Supplementary material online](#).

3.2 *In vitro* assessment: Q_{CFD} predicts absolute flow

Analysis in the 3D printed coronary artery geometries revealed close agreement and correlation between Q_{CFD} and Q_{Exp} (mean delta

+2.08 mL/min, SD 3.45 mL/min, limits of agreement -4.7 to +8.8 mL/min, R^2 0.999; $P < 0.001$) (Figures 3 and 4). Q_{CFD} results were reproducible over three repeated measurements and CFD analyses (CoV <1.0%). When cases with Reynolds numbers >500 were excluded, accuracy improved (mean delta +0.31 mL/min, SD 2.58 mL/min, limits of agreement -4.7 to +5.3 mL/min) (Figure 3). Results for the individual models are provided in the [Supplementary material online](#). The mean CFD processing time for all analyses was 189 s which is tractable for on table clinical decision making.

3.3 Accuracy of Doppler flow

The coefficient of variability for Doppler flow (Q_{Dop}) was 6.4% when the wire was positioned at the inlet, and 17.4% distal to the stenosis. Accordingly, only inlet measurements were considered further. Despite a strong correlation (R^2 0.98; $P < 0.001$), Q_{Dop} underestimated Q_{Exp} (mean delta -14.9 mL/min) and limits of agreement were wider than Q_{CFD} (-48.4 to +18.6 mL/min) (Figure 3). Accuracy of Q_{Dop} was only improved slightly when cases with $Re > 500$ were excluded (mean delta -8.34 mL/min, limits of agreement -36.4 to +19.8 mL/min). Thus, we conclude that in the *in vitro* assessment, the novel Q_{CFD} method

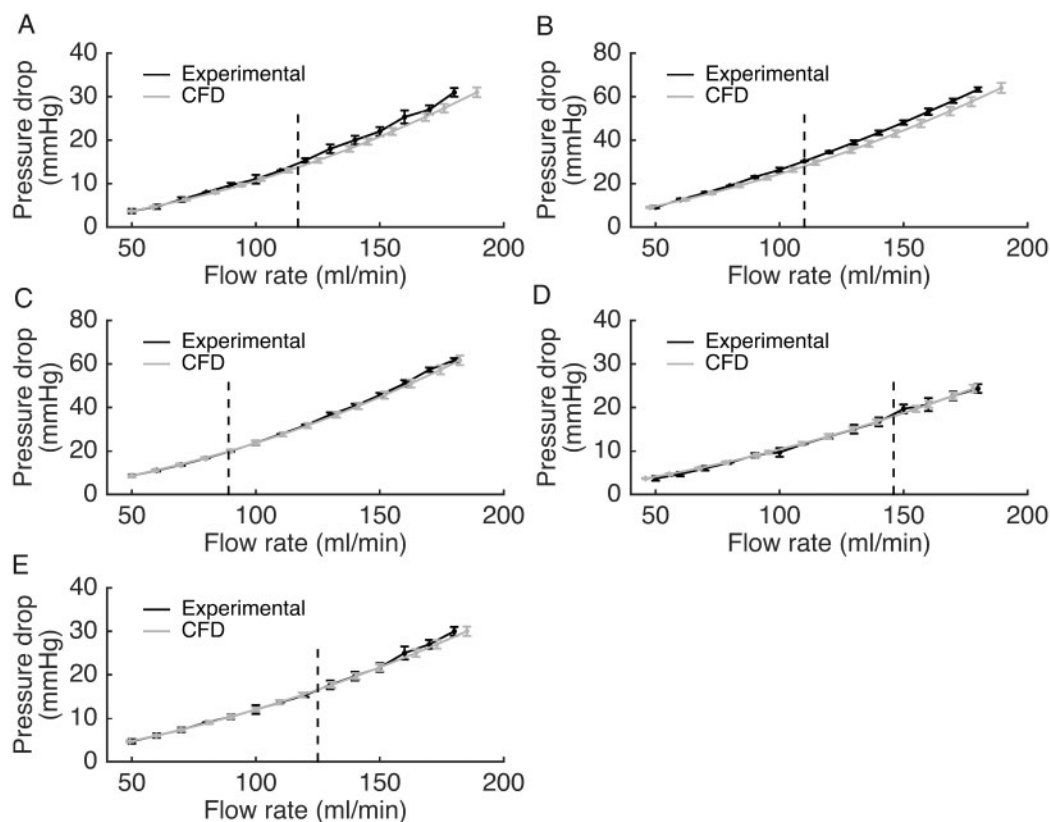


Figure 4 Pressure gradient vs. flow during *in vitro* testing for each of the five models over all flow rates. There was close agreement between the experimental (gold-standard) flow (Q_{exp}) indicated by the black line and the flow rate computed by the novel method (Q_{CFD}) indicated by the grey line (R^2 0.999, $P < 0.001$, by Pearson's correlation coefficient). The vertical dashed line represents the transition between physiological ($Re < 500$) and supra-physiological ($Re \geq 500$) flow rates. For Q_{exp} , error bars represent the maximum and minimum values obtained from three measurements. Because CFD results are inherently reproducible given identical setup parameters, error bars for the Q_{CFD} model were calculated from simulation data representing the influence of small errors in viscosity and density of the experimental blood analogue. Each data point represents the mean of three repeated measurements, i.e. 42 samples per model and 210 all together.

demonstrated close agreement and correlation with the actual flow rate with high reproducibility. Q_{CFD} was considerably more accurate and reproducible than the Doppler wire method.

3.3 First-in-man *in vivo* assessment of Q_{CFD} and MVR

Forty patients were studied during invasive coronary angiography. Mean age was 65 (± 6) years and 86% were male. Medical history included hypertension in 63%, Type 2 diabetes mellitus in 32%, and treated dyslipidaemia in 65%. In total, 13% were current smokers and 5% had experienced prior myocardial infarction. The arteries studied were 29 LAD (72.5%), 5 LCX (12.5%), 5 RCA (12.5%), and 1 left main stem (2.5%). Mean FFR was 0.78 (± 0.12). Q_{CFD} was successfully computed in all cases under baseline and hyperaemic conditions. The mean baseline Q_{CFD} was 62.0 (± 28) mL/min and mean hyperaemic Q_{CFD} was 92.4 (± 46) mL/min. Q_{CFD} was used to additionally calculate coronary MVR, SR and CFR. Between baseline and hyperaemia, there was a 46% reduction in coronary MVR (1.62 ± 0.88 to 0.88 ± 0.45 mmHg·s·mL⁻¹, $P < 0.001$) and a 21% rise in SR (0.19 ± 0.12 to 0.23 ± 0.14 mmHg·s·mL⁻¹, $P < 0.01$). Mean CFR_{QCFD} was 1.56 (± 0.44). Interobserver variability for Q_{CFD} , MVR, and Q_{CFD} -derived CFR was 10%, 11%, and 6%, respectively.

3.4. Accuracy in predicting pressure-derived CFR and reproducing the measured pressure gradient

CFR derived from the novel method (CFR_{QCFD}) correlated closely with pressure-derived CFR ($\text{CFR}_{\text{P-D}}$) (R^2 0.92, $P < 0.001$). $\text{CFR}_{\text{P-D}}$ systematically underestimated CFR_{QCFD} (mean delta -0.16 ± 0.17). The measured and computed physiological parameters of all 40 patients are reported in Table 1. Doppler assessment was attempted in a subset of 20 patients but signal quality was inadequate for CFR estimation in two cases (10%). In the remaining 18, the correlation between CFR derived from Q_{Dop} , (CFR_{Dop}), and $\text{CFR}_{\text{P-D}}$ were weak (R^2 0.32, $P = 0.1$). Similar to CFR_{QCFD} , CFR_{Dop} also overestimated $\text{CFR}_{\text{P-D}}$ (mean delta -0.35 ± 0.46). When the computational model was reversed to apply flow at the inlet, application of Q_{CFD} accurately predicted the invasively measured pressure gradients (bias -0.29 , SD 0.46 mmHg, limits of agreement -1.19 to $+0.61$ mmHg), whereas Q_{Dop} consistently underestimated the invasively measured pressure gradient (bias -8.93 , SD 12.46 mmHg limits of agreement -33.35 to $+15.49$ mmHg). Unlike the *in vitro* experiments, this does not provide a rigorous validation of flow results, but it does suggest that the Q_{CFD} method was reasonably accurate relative to Doppler. Figure 5 demonstrates a screenshot of a result within the virtuQ software environment.

Table 1 Measured and computed physiological parameters for all 40 cases

Case	Artery	Baseline						Hyperaemic						BL-Hyp % delta			CFR				
		No	Pa	Pd	dP	Pd/Pa	Q_CFD	MVR	SR	Pa	Pd	dP	FFR	Q_CFD	MVR	SR	MVR	SR	Q	Dop	Q_CFD
1	LAD	88.0	79.4	8.7	0.90	22.7	3.49	0.38	78.0	61.0	17.0	0.78	35.8	1.70	0.47	-51	24	58	1.8	1.58	1.40
2	LAD	92.7	85.6	7.1	0.92	67.7	1.26	0.10	75.7	61.5	14.2	0.81	109.2	0.56	0.13	-56	30	61	1.3	1.61	1.41
3	RCA	106.3	99.6	6.7	0.94	89.8	1.11	0.08	83.5	71.3	12.2	0.85	165.3	0.43	0.07	-61	-13	84	2.1	1.84	1.35
4	LAD	119.9	114.7	5.1	0.96	72.9	1.57	0.07	114.9	91.7	23.1	0.80	193.0	0.48	0.12	-69	71	165	2.4	2.65	2.13
5	RCA	89.1	66.4	22.7	0.74	93.2	0.71	0.24	88.3	53.8	34.5	0.61	121.9	0.44	0.28	-38	17	31	1.5	1.31	1.23
6	LCX	74.3	69.1	5.2	0.93	36.6	1.89	0.14	77.4	60.0	17.5	0.77	88.7	0.68	0.20	-64	43	142	1.1	2.42	1.83
7	LAD	76.7	51.8	24.9	0.68	89.0	0.58	0.28	65.2	33.1	32.2	0.51	105.4	0.31	0.31	-47	11	19	1.1	1.19	1.14
8	LAD	99.0	80.9	18.1	0.82	75.4	1.07	0.24	104.6	73.6	31.0	0.70	108.9	0.68	0.28	-36	17	44	1.5	1.44	1.31
9	LAD	96.4	87.6	8.8	0.91	36.6	2.40	0.24	71.4	62.7	8.7	0.88	36.3	1.73	0.24	-28	0	-1	2.40	0.99	0.99
10	LAD	117.3	112.9	4.4	0.96	23.5	4.80	0.19	102.3	89.0	13.3	0.87	52.8	1.69	0.25	-65	32	125	2.07	2.25	1.74
11	RCA	90.0	88.0	1.9	0.98	41.3	2.13	0.05	75.0	67.6	7.4	0.90	102.5	0.66	0.07	-69	40	148	1.90	2.48	1.97
12	RCA	112.1	59.4	52.7	0.53	115.1	0.52	0.46	118.8	62.2	56.5	0.52	119.7	0.52	0.47	0	2	4	1.18	1.04	1.04
13	LAD	112.6	106.9	5.7	0.95	58.0	1.84	0.10	110.4	103.4	7.0	0.94	66.4	1.56	0.11	-15	10	14	1.38	1.14	1.11
14	RCA	106.5	105.8	0.7	0.99	29.7	3.56	0.02	103.7	102.0	1.7	0.98	60.1	1.70	0.03	-52	50	102	2.42	2.02	1.56
15	LAD	99.6	80.3	19.3	0.81	46.4	1.73	0.42	97.0	69.9	27.1	0.72	58.2	1.20	0.47	-31	12	25	1.61	1.25	1.18
16	LAD	109.9	92.9	17	0.85	86.8	1.07	0.20	103.1	86.1	17.0	0.84	86.7	0.99	0.20	-7	0	0	1.67	1.00	1.00
17	LAD	110.3	98.4	11.9	0.89	55.6	1.68	0.21	106.4	85.0	21.4	0.80	79.1	1.01	0.27	-40	29	42	1.2	1.42	1.34
18	LCX	108.1	94.5	13.6	0.87	85.0	1.05	0.16	113.7	88.5	25.2	0.78	121.2	0.69	0.21	-34	31	43	2	1.43	1.36
19	LAD	96.4	87.6	8.8	0.91	84.1	0.98	0.10	71.5	62.4	9.1	0.87	85.2	0.67	0.11	-32	10	1	F	1.01	1.02
20	LAD	106.3	99.6	6.7	0.94	67.6	1.40	0.10	81.8	63.6	18.2	0.78	123.5	0.47	0.15	-66	50	83	F	1.83	1.65
21	LAD	88.6	79.5	9.1	0.90	27.1	2.75	0.34	80.9	58.9	22.0	0.73	47.7	1.13	0.46	-59	35	76		1.76	1.55
22	LAD	74.4	49.5	24.9	0.67	56.2	0.83	0.44	65.0	32.9	32.1	0.51	65.8	0.43	0.49	-48	11	17		1.17	1.14
23	LCX	73.6	68.3	5.3	0.93	38.7	1.64	0.14	79.1	60.8	18.3	0.77	81.6	0.68	0.22	-59	57	111		2.11	1.86
24	LAD	96.3	87.5	8.8	0.91	41.0	2.01	0.21	71.5	62.4	9.1	0.87	41.1	1.40	0.22	-30	5	0		1.00	1.02
25	LAD	99.0	80.9	18.1	0.82	57.4	1.32	0.32	104.4	73.5	30.9	0.70	79.8	0.86	0.39	-35	22	39		1.39	1.31
26	LAD	119.0	112.1	6.9	0.94	42.0	2.55	0.16	103.4	88.5	14.9	0.86	62.6	1.33	0.24	-48	50	49		1.49	1.47
27	LAD	112.3	106.7	5.6	0.95	61.5	1.65	0.09	122.0	113.1	8.9	0.93	82.2	1.32	0.11	-20	22	34		1.34	1.26
28	LAD	99.6	80.3	19.3	0.81	47.3	1.59	0.41	95.5	68.7	26.8	0.72	58.8	1.09	0.46	-31	12	24		1.24	1.18
29	LMS	78.8	64.7	14.1	0.82	169.4	0.35	0.08	75.3	47.4	27.9	0.63	257.4	0.16	0.11	-54	38	52		1.52	1.41
30	LAD	87.0	82.1	4.9	0.94	43.4	1.78	0.11	84.1	70.9	13.2	0.84	79.5	0.83	0.17	-53	55	83		1.83	1.64
31	LAD	81.5	73.0	8.5	0.90	44.1	1.54	0.19	78.3	58.2	20.1	0.74	78.2	0.68	0.26	-56	37	77		1.77	1.54
32	LAD	101.6	84.4	17.2	0.83	38.2	2.08	0.45	82.5	48.2	34.3	0.58	59.7	0.72	0.57	-65	27	56		1.56	1.41
33	LAD	93.5	86.3	7.2	0.92	79.4	0.97	0.12	87.0	62.0	25.0	0.71	148.7	0.38	0.17	-61	42	87		1.87	1.86
34	LAD	109.0	102.0	7.0	0.94	52.4	1.85	0.13	118.8	110.2	8.6	0.93	59.0	1.78	0.15	-4	15	13		1.13	1.11
35	LCX	130.4	119.4	11.0	0.92	79.6	1.44	0.14	118.0	101.0	17.0	0.86	105.2	0.91	0.16	-37	14	32		1.32	1.24
36	LCX	94.2	84.9	9.3	0.90	83.4	0.96	0.11	96.7	67.6	29.1	0.70	173.8	0.36	0.17	-63	55	108		2.08	1.77
37	LAD	99.7	90.5	9.2	0.91	75.1	1.14	0.12	98.2	84.8	13.4	0.86	92.5	0.86	0.14	-25	17	23		1.23	1.21
38	LAD	88.0	82.6	5.4	0.94	66.8	1.16	0.08	78.7	58.6	20.1	0.74	138.1	0.39	0.15	-66	88	107		2.07	1.93
39	LAD	67.1	59.8	7.3	0.89	50.4	1.09	0.14	69.8	59.4	10.4	0.85	63.7	0.85	0.16	-22	14	26		1.26	1.19
40	LAD	69.8	64.4	5.4	0.92	49.7	1.20	0.11	66.0	56.1	9.9	0.85	73.9	0.69	0.13	-43	18	49		1.49	1.35

BL, baseline; CFR, coronary flow reserve; Dop, Doppler; F, failed; FFR, fractional flow reserve; Hyp, hyperaemia; LAD, left anterior descending; LCX, left circumflex; LMS, left main stem; MVR, microvascular resistance; Pa, proximal pressure; Pd, distal pressure; P-D, pressure derived; Q_CFD, coronary flow computed by the novel method; RCA, right coronary artery; SR, stenosis resistance.

4. Discussion

In this study, we have demonstrated that absolute coronary blood flow can be determined from data generated during standard angiography and pressure wire assessment. In addition to absolute coronary flow, FFR, MVR, SR, and CFR can be determined simultaneously, providing a comprehensive physiological assessment of the key physiological parameters which characterize the entire coronary circulation. Uniquely, the method does not require any dedicated hardware, infusions or

interventional effort. The novel method was more accurate and reproducible than the Doppler wire technique.

Indices of translesional pressure ratio like FFR and iFR are themselves methods for deriving flow from pressure and are superior to angiography in determining physiological lesion significance. However, flow is not measured, but inferred, based upon a number of assumptions. These indices reflect percentage changes in flow, of an unknown value, relative to a hypothetical norm. We propose there is value in understanding flow and flow reduction in absolute terms. An FFR of 0.75 indicates a 25%

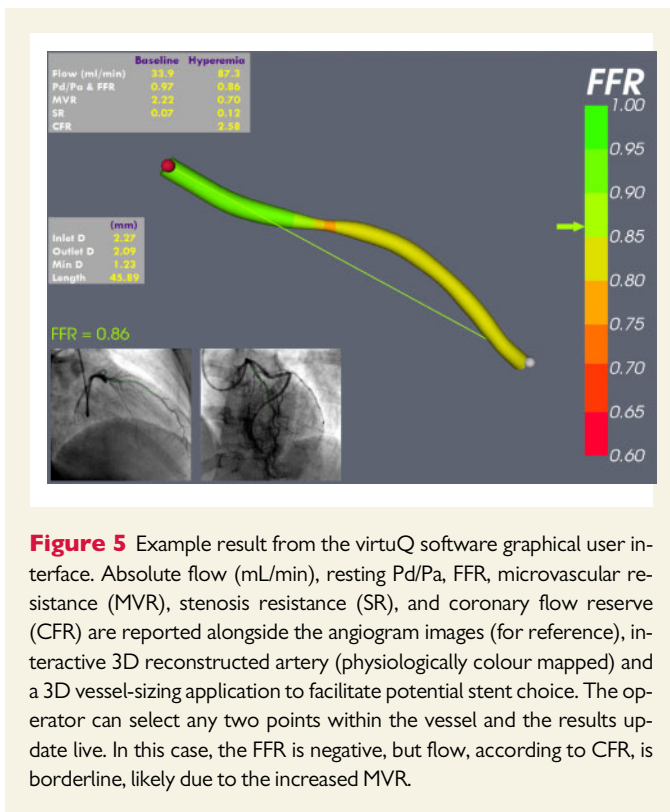


Figure 5 Example result from the virtuQ software graphical user interface. Absolute flow (mL/min), resting Pd/Pa, FFR, microvascular resistance (MVR), stenosis resistance (SR), and coronary flow reserve (CFR) are reported alongside the angiogram images (for reference), interactive 3D reconstructed artery (physiologically colour mapped) and a 3D vessel-sizing application to facilitate potential stent choice. The operator can select any two points within the vessel and the results update live. In this case, the FFR is negative, but flow, according to CFR, is borderline, likely due to the increased MVR.

reduction of flow in that artery, compared with the undiseased state. Precisely how much blood flow this is cannot be known. This may be an important limitation, because an FFR of 0.75 in a diagonal branch may represent just a few mL/min of flow reduction, whereas the same FFR in a proximal LAD may indicate well over 100 mL/min flow reduction. Similarly, an FFR 0.78 in the diagonal branch might seem to mandate PCI, whereas an FFR of 0.82 in a proximal LAD would not, even if, in absolute terms, the LAD lesion is associated with a far greater reduction in absolute myocardial blood flow. The value of FFR is that it has allowed interventionists to begin to quantify blood flow reduction in the catheter laboratory, but the ability to accurately quantify coronary blood flow changes in absolute terms may enable a more refined and patient-specific approach to coronary physiological assessment and treatment decisions. Without any additional equipment than it takes to measure FFR, our novel computational method additionally reports (i) the flow reduction in absolute terms, (ii) the MVR, (iii) the SR, and (iv) the CFR. Thus, the new method does not compete with traditional parameters like FFR or iFR, but instead complements and augments them, providing a new level of coronary physiological information. Our method took between seven and eight minutes to complete using our software; four to five min to reconstruct the arterial geometry and three to compute the physiology. Speed of computation was not the focus of this study, rather accuracy of the novel method. We anticipate results can be achieved in less than 5 min with development of the user interface and accelerated CFD code.

An important advantage of the novel method is that it provides information regarding microvascular disease. The importance of MVD is increasingly being recognized. The coronary microvasculature holds 90% of the total myocardial blood volume.²⁰ MVD is implicated in angina with no obstructive coronary disease, also known as 'syndrome X' or microvascular angina, which can lead to ventricular dysfunction even in those

with normal epicardial arteries. A recent study demonstrated evidence of coronary MVD in 68% of those attending the catheter laboratory with chest pain with no obstructive coronary disease and 39–53% of those with concomitant epicardial disease.²¹ MVD is of prognostic importance in acute myocardial infarction,²² myocardial infarction with no obstructive coronary artery disease,²³ cardiomyopathy,^{24,25} cardiac transplantation,²⁶ and heart failure with preserved ejection fraction.²⁷ A recent randomized controlled trial demonstrated that coronary MVD responds well to stratified medical therapy.⁹ It is also hypothesized that coronary MVD may help to explain excess symptoms, risk and major adverse cardiac event in women,²⁸ and the roughly 20% rate of persistent angina despite epicardial revascularization with PCI.^{29–31} Because routine invasive testing with angiography and pressure-derived FFR/iFR overlook the microvascular physiology, virtuQ may have a valuable role in providing the necessary additional parameters to better characterize coronary pathophysiology, improve diagnosis of MVD and better stratify treatment in these patients.

Because IHD results from a reduction in coronary blood flow, developing a method for measuring flow has been a scientific goal for many years. Until recently, this has meant using Doppler ultrasound or thermodilution but these indirect measures have proved impractical, technically challenging and inaccurate and have not been adopted into routine practice.^{32–35} The challenges of maintaining an optimum Doppler signal are well documented^{36–38} and the drawbacks widely acknowledged, even by those who advocate incorporating flow into physiological coronary assessment.^{17,38–40} Misalignment of the transducer may underestimate flow velocity. This was observed in the current study despite painstaking positioning *in vitro*. Doppler signal is sensitive to small movements and artefact is common.^{36,39} Whilst these errors may 'cancel out' in the calculation of CFR (ratio of two velocities), indices such as hyperaemic SR ($HSR = P_d/\text{Doppler velocity}$) are far more susceptible to these errors. Kousera et al.¹⁷ used CFD simulation to predict the pressure-flow relationship in patients with coronary disease but underestimated pressure drop, likely because of error in the Doppler measurements, upon which their model was critically dependent. CFR is somewhat resistant to these errors if the magnitude of baseline and hyperaemic error remain unchanged. Indices such as hyperaemic or baseline SR ($\frac{P_a - P_d}{APV}$), hyperaemic myocardial resistance ($\frac{P_d}{APV}$) and index of myocardial resistance ($P_d \cdot \text{mean transit time}$) are far more susceptible to error in the Doppler- or thermodilution-derived flow estimation. Recently, an improved thermodilution method has been introduced that uses a mono-rail infusion catheter and a thermo- and pressure-sensitive wire.^{41–43} This method can measure absolute flow and MVR but requires dedicated hardware, reports hyperaemic flow at the catheter location and is associated with wider limits of agreement than the Q_{CFD} method (-37 to +24 vs. -4.7 to +8.8 mL/min), although the authors acknowledge that the virtuQ method is at an earlier stage of development and testing. We believe virtuQ to be the first non-Doppler and non-thermodilution invasive method for predicting coronary flow to be described.

Pressure-derived CFR is known to correlate closely with CFR derived from absolute flow as originally demonstrated in a canine model by Akasaka et al.¹⁸ In this study, CFR derived from Q_{CFD} correlated closely with pressure-derived CFR, suggesting Q_{CFD} was an accurate measure of absolute coronary flow. While the correlation was strong, CFR derived from Q_{CFD} was consistently greater than pressure-derived CFR. This is interesting and reassuring because the same observation was made by MacCarthy et al.⁴⁴ in their experiment comparing thermo- and Doppler-derived CFR to pressure-derived CFR. The discrepancy is likely

explained by the fact that the calculation of pressure-derived CFR neglects frictional energy losses, which our method fully captures.

Clinical data required for the virtuQ method are angiographic images and standard pressure-wire measurements, methods with which interventionists are already routinely familiar. Standard pressure wires tend to have better handling characteristics than those with combined Doppler or thermosensitive transducers. virtuQ requires no additional hardware, wires or infusions. A comprehensive physiological and anatomical assessment is generated (FFR, Q_{CFD} , MVR, SR, and CFR) under baseline and hyperaemic conditions and this can be visualized in a user-friendly software environment. Whereas existing techniques estimate surrogate markers of flow (e.g. velocity or mean transit time) and incorporate these into ratios or indices, virtuQ determines flow and resistance in absolute units.

CFD modelling is increasingly being applied to cardiovascular medicine to characterize and predict human vascular pathophysiology which is poorly approximated by simpler fluid dynamic equations such as those of Bernoulli and Poiseuille.^{14,44,45} Perhaps the best example is virtual FFR (vFFR) computed from angiography. The accuracy of any CFD model is critically dependent upon tuning parameters that represent the physiological conditions of an individual patient, i.e. boundary conditions.^{46–48} When computing vFFR, the boundary conditions are unknown and assumptions have to be made. This limits accuracy. This is not a problem for virtuQ because the boundary conditions are known precisely in all cases. Thus, assumptions and therefore error are reduced.

4.1 Limitations

In the *in vitro* experiment, the 3D printed coronary models were rigid. The same is true of the computational model. However, we expect the overall effect coronary compliance to be negligible, especially in the context of a steady flow simulation and diseased vessels. Furthermore, previous CFD modelling work suggests a rigid assumption is acceptable in this context and does not adversely affect accuracy.^{14,49–51} At the current stage of development, the model does not account for flow to side branches which underestimates flow in more proximal segments. This is the opposite of the over-the-wire catheter infusion method because this predicts proximal but not distal flow. Future work will improve this by quantifying the flow lost to proximal branches. Because the simulation boundary conditions are known precisely, Q_{CFD} accuracy is dependent chiefly on the reconstruction protocol. In this study, we evaluated Doppler, as a clinically approved comparator, and found it lacking; a similar evaluation of thermodilution derived markers of flow would also be valuable.⁴² A potential limitation of the Q_{CFD} method as a clinical tool is the requirement for a pressure gradient of at least 4 mmHg in the epicardial artery to drive the CFD simulation. Theoretically, this means Q_{CFD} cannot be used in completely normal coronary arteries. Assuming a mean arterial pressure of 90 mmHg, Q_{CFD} will be accurate in cases where FFR is ≤ 0.95 , i.e. the majority of cases studied in the catheter laboratory. This will affect baseline measurements more than hyperaemic. Ideally, coronary flow would be interpreted in light of the mass of myocardium subtended by that artery. However, there are currently no methods for measuring this in the cardiac catheter laboratory. Non-invasive techniques such as PET or CMR may have a role but are imprecise concerning the location of a stenosis.

5. Conclusions

Absolute coronary blood flow can be determined during standard angiography and pressure wire assessment. This novel method provides a comprehensive coronary physiological assessment of flow, pressure and resistance, across the entire coronary circulation, without the need for additional hardware, catheters, wires, or infusions. Using the novel method, epicardial and microvascular disease can be discriminated and quantified.

Data availability

The data underlying this article are available in the article and in its online [supplementary material](#).

Supplementary material

[Supplementary material](#) is available at *Cardiovascular Research* online.

Authors' contributions

All authors made a substantial contribution either to the conception or design of the work (P.D.M., A.J.N., R.D.H., I.Z., P.V.L.), the acquisition and/or analysis of data (I.Z., H.E., L.A.-R., R.G., K.C., P.D.M.), interpretation of data (P.D.M., A.J.N., H.E., I.Z.), drafting the work (P.D.M., A.J.N., P.V.L., R.G.), or revising the work critically for important intellectual content (P.C.E.).

Acknowledgements

The authors are grateful to Dr Michel Rochette at ANSYS Inc. for his support with the CFD processing, and to the radiographers and cardiac physiologists at Sheffield Teaching Hospitals for their support in collecting the imaging and physiological data.

Conflict of interest: none declared.

Funding

P.D.M. was funded by a Wellcome Trust Clinical Research Career Development Fellowship (214567/Z/18/Z). This work was supported by a UK Medical Research Council Confidence in Concepts grant (R/005998-13-44). P.D.M. and R.G. were previously funded by British Heart Foundation Clinical Research Training Fellowships (FS/12/85/29869 and FS/16/48/32306). P.C.E. was funded by the British Heart Foundation, UK (RG/19/10/34506)..

References

- Pijls NH, De Bruyne B, Peels K, Van Der Voort PH, Bonnier HJ, Bartunek J, Koolen JJ. Measurement of fractional flow reserve to assess the functional severity of coronary-artery stenoses. *N Engl J Med* 1996;**334**:1703–1708.
- De Bruyne B, Pijls NH, Kalesan B, Barbato E, Tonino PA, Piroth Z, Jagic N, Mobius-Winckler S, Rioufol G, Witt N, Kala P, MacCarthy P, Engstrom T, Oldroyd KG, Mavromatis K, Manoharan G, Verlee P, Frobert O, Curzen N, Johnson JB, Juni P, Fearon WF; FAME 2 Trial Investigators. Fractional flow reserve-guided PCI versus medical therapy in stable coronary disease. *N Engl J Med* 2012;**367**:991–1001.
- Gotberg M, Christiansen EH, Gudmundsdottir JJ, Sandhall L, Danielewicz M, Jakobsen L, Olsson SE, Ohagen P, Olsson H, Omerovic E, Calais F, Lindroos P, Maeng M, Todt T, Venetsanos D, James SK, Karegren A, Nilsson M, Carlsson J, Hauer D, Jensen J, Karlsson AC, Panayi G, Erlinge D, Frobert O, Frsi I. Instantaneous wave-free ratio versus fractional flow reserve to guide PCI. *N Engl J Med* 2017;**376**:1813–1823.

4. Carrick D, Haig C, Ahmed N, Carberry J, Yue May VT, McEntegart M, Petrie MC, Eteiba H, Lindsay M, Hood S, Watkins S, Davie A, Mahrous A, Mordi I, Ford I, Radjenovic A, Oldroyd KG, Berry C. Comparative prognostic utility of indexes of microvascular function alone or in combination in patients with an acute ST-segment-elevation myocardial infarction. *Circulation* 2016;**134**:1833–1847.
5. Martinez GJ, Yong AS, Fearon WF, Ng MK. The index of microcirculatory resistance in the physiologic assessment of the coronary microcirculation. *Coron Artery Dis* 2015; **26**(Suppl 1):e15–e26.
6. Crea F, Bairey Merz CN, Beltrame JF, Kaski JC, Ogawa H, Ong P, Sechtem U, Shimokawa H, Camici PG; Coronary Vasomotion Disorders International Study Group (COVADIS). The parallel tales of microvascular angina and heart failure with preserved ejection fraction: a paradigm shift. *Eur Heart J* 2017;**38**:473–477.
7. Shome JS, Perera D, Plein S, Chiribiri A. Current perspectives in coronary microvascular dysfunction. *Microcirculation* 2017;**24**:e12340.
8. Crea F, Camici PG, Bairey Merz CN. Coronary microvascular dysfunction: an update. *Eur Heart J* 2014;**35**:1101–1111.
9. Ford TJ, Stanley B, Good R, Rocchiccioli P, McEntegart M, Watkins S, Eteiba H, Shaikat A, Lindsay M, Robertson K, Hood S, McGeoch R, McDade R, Yui E, Sidik N, McCartney P, Corcoran D, Collison D, Rush C, McConnachie A, Touyz RM, Oldroyd KG, Berry C. Stratified medical therapy using invasive coronary function testing in angina: the CorMicA trial. *J Am Coll Cardiol* 2018;**72**:2841–2855.
10. Shaw LJ, Berman DS, Maron DJ, Mancini GBJ, Hayes SW, Hartigan PM, Weintraub WS, O'Rourke RA, Dada M, Spertus JA, Chaitman BR, Friedman J, Slomka P, Heller GV, Germano G, Gosselin G, Berger P, Kostuk WJ, Schwartz RG, Knudtson M, Veledar E, Bates ER, McCallister B, Teo KK, Boden WE. Optimal medical therapy with or without percutaneous coronary intervention to reduce ischemic burden: results from the Clinical Outcomes Utilizing Revascularization and Aggressive Drug Evaluation (COURAGE) trial nuclear substudy. *Circulation* 2008;**117**:1283–1291.
11. Xaplanteris P, Fournier S, Pijls NHJ, Fearon WF, Barbato E, Tonino PAL, Engstrom T, Kaab S, Dambink JH, Rioufol G, Toth GG, Piroth Z, Witt N, Frobert O, Kala P, Linke A, Jagic N, Mates M, Mavromatis K, Samady H, Irimpen A, Oldroyd K, Campo G, Rothenbuehler M, Juni P, De Bruyne B; FAME 2 Investigators. Five-year outcomes with PCI guided by fractional flow reserve. *N Engl J Med* 2018;**379**:250–259.
12. Morris PD, Silva Soto DA, Feher JFA, Rafiroiu D, Lungu A, Varma S, Lawford PV, Hose DR, Gunn JP. Fast virtual fractional flow reserve based upon steady-state computational fluid dynamics analysis: results from the VIRTU-fast study. *JACC Basic Transl Sci* 2017;**2**:434–446.
13. Gosling RC, Morris PD, Silva Soto DA, Lawford PV, Hose DR, Gunn JP. Virtual coronary intervention: a treatment planning tool based upon the angiogram. *JACC Cardiovasc Imaging* 2019;**12**:865–872.
14. Morris PD, Narracott A, von Tengge-Koblogk H, Silva Soto DA, Hsiao S, Lungu A, Evans P, Bressloff NW, Lawford PV, Hose DR, Gunn JP. Computational fluid dynamics modelling in cardiovascular medicine. *Heart* 2016;**102**:18–28.
15. Segur JA, Oberstar HE. Viscosity of glycerol and its aqueous solutions. *Ind Eng Chem* 1951;**43**:2117–2120.
16. Samavat H, Evans JA. An ideal blood mimicking fluid for doppler ultrasound phantoms. *J Med Phys* 2006;**31**:275–278.
17. Kousera CA, Nijjer S, Torii R, Petraco R, Sen S, Foin N, Hughes AD, Francis DP, Xu XY, Davies JE. Patient-specific coronary stenoses can be modeled using a combination of OCT and flow velocities to accurately predict hyperemic pressure gradients. *IEEE Trans Biomed Eng* 2014;**61**:1902–1913.
18. Akasaka T, Yamamuro A, Kamiyama N, Koyama Y, Akiyama M, Watanabe N, Neishi Y, Takagi T, Shalman E, Barak C, Yoshida K. Assessment of coronary flow reserve by coronary pressure measurement: comparison with flow- or velocity-derived coronary flow reserve. *J Am Coll Cardiol* 2013;**61**:1554–1560.
19. Bland JM, Altman DG. Statistical methods for assessing agreement between two methods of clinical measurement. *Lancet* 1986;**327**:307–310.
20. Herrmann J, Kaski JC, Lerman A. Coronary microvascular dysfunction in the clinical setting: from mystery to reality. *Eur Heart J* 2012;**33**:2771–2782b.
21. Corcoran D, Young R, Adlam D, McConnachie A, Mangion K, Ripley D, Cairns D, Brown J, Bucciarelli-Ducci C, Baumbach A, Kharbanda R, Oldroyd KG, McCann GP, Greenwood JP, Berry C. Coronary microvascular dysfunction in patients with stable coronary artery disease: the CE-MARC 2 coronary physiology sub-study. *Int J Cardiol* 2018;**266**:7–14.
22. Fearon WF, Low AF, Yong AS, McGeoch R, Berry C, Shah MG, Ho MY, Kim HS, Loh JP, Oldroyd KG. Prognostic value of the index of microcirculatory resistance measured after primary percutaneous coronary intervention. *Circulation* 2013;**127**:2436–2441.
23. Germing A, Lindstaedt M, Ulrich S, Grewe P, Bojara W, Lawo T, von Dryander S, Jager D, Machraoui A, Mugge A, Lemke B. Normal angiogram in acute coronary syndrome—preangiographic risk stratification, angiographic findings and follow-up. *Int J Cardiol* 2005;**99**:19–23.
24. Neglia D, Michelassi C, Trivieri MG, Sambucetti G, Giorgetti A, Pratali L, Gallopin M, Salvadori P, Sorace O, Carpeggiani C, Poddighe R, L'Abbate A, Parodi O. Prognostic role of myocardial blood flow impairment in idiopathic left ventricular dysfunction. *Circulation* 2002;**105**:186–193.
25. Cecchi F, Olivetto I, Gistri R, Lorenzoni R, Chiriatti G, Camici PG. Coronary microvascular dysfunction and prognosis in hypertrophic cardiomyopathy. *N Engl J Med* 2003;**349**:1027–1035.
26. Tona F, Caforio AL, Montisci R, Gambino A, Angelini A, Ruscazio M, Toscano G, Feltrin G, Ramondo A, Gerosa G, Iliceto S. Coronary flow velocity pattern and coronary flow reserve by contrast-enhanced transthoracic echocardiography predict long-term outcome in heart transplantation. *Circulation* 2006;**114**:I-49–I-55.
27. Taqueti VR, Solomon SD, Shah AM, Desai AS, Groarke JD, Osborne MT, Hainer J, Bibbo CF, Dorbala S, Blankstein R, Di Carli MF. Coronary microvascular dysfunction and future risk of heart failure with preserved ejection fraction. *Eur Heart J* 2018;**39**:840–849.
28. Vaccarino V, Badimon L, Corti R, de Wit C, Dorobantu M, Hall A, Koller A, Marzilli M, Pries A, Bugiardini R; Working Group on Coronary Pathophysiology and Microcirculation. Ischaemic heart disease in women: are there sex differences in pathophysiology and risk factors? Position paper from the working group on coronary pathophysiology and microcirculation of the European Society of Cardiology. *Cardiovasc Res* 2011;**90**:9–17.
29. Stergiopoulos K, Boden WE, Hartigan P, Mobius-Winkler S, Hambrecht R, Hueb W, Hardison RM, Abbott JD, Brown DL. Percutaneous coronary intervention outcomes in patients with stable obstructive coronary artery disease and myocardial ischemia: a collaborative meta-analysis of contemporary randomized clinical trials. *JAMA Intern Med* 2014;**174**:232–240.
30. Izzo P, Macchi A, De Gennaro L, Gaglione A, Di Biase M, Brunetti ND. Recurrent angina after coronary angioplasty: mechanisms, diagnostic and therapeutic options. *Eur Heart J Acute Cardiovasc Care* 2012;**1**:158–169.
31. Kim MC, Kini A, Sharma SK. Refractory angina pectoris: mechanism and therapeutic options. *J Am Coll Cardiol* 2002;**39**:923–934.
32. Cole JS, Hartley CJ. The pulsed Doppler coronary artery catheter preliminary report of a new technique for measuring rapid changes in coronary artery flow velocity in man. *Circulation* 1977;**56**:18–25.
33. Wilson RF, Laughlin DE, Ackell PH, Chilian WM, Holida MD, Hartley CJ, Armstrong ML, Marcus ML, White CV. Transluminal, subselective measurement of coronary artery blood flow velocity and vasodilator reserve in man. *Circulation* 1985;**72**:82–92.
34. Sibley DH, Millar HD, Hartley CJ, Whitlow PL. Subselective measurement of coronary blood flow velocity using a steerable Doppler catheter. *J Am Coll Cardiol* 1986;**8**:1332–1340.
35. Barbato E, Aarnoudse W, Aengevaeren WR, Werner G, Klaus V, Bojara W, Herzfeld I, Oldroyd KG, Pijls NH, De BB. Validation of coronary flow reserve measurements by thermodilution in clinical practice. *Eur Heart J* 2004;**25**:219–223.
36. Kern MJ. Coronary physiology revisited: practical insights from the cardiac catheterization laboratory. *Circulation* 2000;**101**:1344–1351.
37. Siebes M, Verhoeff BJ, Meuwissen M, de Winter RJ, Spaan JA, Piek JJ. Single-wire pressure and flow velocity measurement to quantify coronary stenosis hemodynamics and effects of percutaneous interventions. *Circulation* 2004;**109**:756–762.
38. van de Hoef TP, Nolte F, Damman P, Delewi R, Bax M, Chamuleau SA, Voskuil M, Siebes M, Tijssen JG, Spaan JA, Piek JJ, Meuwissen M. Diagnostic accuracy of combined intracoronary pressure and flow velocity information during baseline conditions: adenosine-free assessment of functional coronary lesion severity. *Circ Cardiovasc Interv* 2012;**5**:508–514.
39. Kern MJ, Lerman A, Bech JW, De Bruyne B, Eeckhout E, Fearon WF, Higano ST, Lim MJ, Meuwissen M, Piek JJ, Pijls NH, Siebes M, Spaan JA. Physiological assessment of coronary artery disease in the cardiac catheterization laboratory: a scientific statement from the American Heart Association Committee on Diagnostic and Interventional Cardiac Catheterization, Council on Clinical Cardiology. *Circulation* 2006;**114**:1321–1341.
40. van de Hoef TP, Siebes M, Spaan JA, Piek JJ. Fundamentals in clinical coronary physiology: why coronary flow is more important than coronary pressure. *Eur Heart J* 2015;**36**:3312–3319.
41. Aarnoudse W, van't Veer M, Pijls NHJ, ter Woorst J, Vercauteren S, Tonino P, Geven M, Rutten M, van Hagen E, de Bruyne B, van de Vosse F. Direct volumetric blood flow measurement in coronary arteries by thermodilution. *J Am Coll Cardiol* 2007;**50**:2294–2304.
42. van't Veer M, Adedji J, Wijnbergen I, Tóth GG, Rutten MCM, Barbato E, van Nunen LX, Pijls NHJ, De Bruyne B. Novel monorail infusion catheter for volumetric coronary blood flow measurement in humans: *in vitro* validation. *EuroIntervention* 2016;**12**:701–707.
43. Xaplanteris P, Fournier S, Keulards DCJ, Adedji J, Ciccarelli G, Milkas A, Pellicano M, van't Veer M, Barbato E, Pijls NHJ, De Bruyne B. Catheter-based measurements of absolute coronary blood flow and microvascular resistance: feasibility, safety, and reproducibility in humans. *Circ Cardiovasc Interv* 2018;**11**:e006194.
44. MacCarthy P, Berger A, Manoharan G, Bartunek J, Barbato E, Wijns W, Heyndrickx GR, Pijls NHJ, De Bruyne B. Pressure-derived measurement of coronary flow reserve. *J Am Coll Cardiol* 2005;**45**:216–220.
45. Morris PD, Curzen N, Gunn JP. Angiography-derived fractional flow reserve: more or less physiology? *J Am Heart Assoc* 2020;**9**:e015586.
46. Taylor CA, Fonte TA, Min JK. Computational fluid dynamics applied to cardiac computed tomography for noninvasive quantification of fractional flow reserve: scientific basis. *J Am Coll Cardiol* 2013;**61**:2233–2241.
47. Morris PD, Ryan D, Morton AC, Lycett R, Lawford PV, Hose DR, Gunn JP. Virtual fractional flow reserve from coronary angiography: modeling the significance of

- coronary lesions: results from the VIRTU-1 (VIRTUal Fractional Flow Reserve From Coronary Angiography) study. *JACC Cardiovasc Interv* 2013;**6**:149–157.
48. Morris PD, van de Vosse FN, Lawford PV, Hose DR, Gunn JP. "Virtual" (Computed) fractional flow reserve: current challenges and limitations. *JACC Cardiovasc Interv* 2015;**8**:1009–1017.
49. Brown AG, Shi Y, Marzo A, Staicu C, Valverde I, Beerbaum P, Lawford PV, Hose DR. Accuracy vs. computational time: translating aortic simulations to the clinic. *J Biomech* 2012;**45**:516–523.
50. Zeng D, Boutsianis E, Ammann M, Boomsma K, Wildermuth S, Poulidakos D. A study on the compliance of a right coronary artery and its impact on wall shear stress. *J Biomech Eng* 2008;**130**:041014.
51. Xu B, Tu S, Qiao S, Qu X, Chen Y, Yang J, Guo L, Sun Z, Li Z, Tian F, Fang W, Chen J, Li W, Guan C, Holm NR, Wijns W, Hu S. Diagnostic accuracy of angiography-based quantitative flow ratio measurements for online assessment of coronary stenosis. *J Am Coll Cardiol* 2017;**70**:3077–3087.

Translational perspective

Current pressure wire-based methods of assessing coronary disease cannot assess absolute flow or microvascular disease. Our novel absolute coronary flow (Q_{CFD}) method, using only angiography-based computational fluid dynamics and a pressure wire, simultaneously measures fractional flow reserve, absolute coronary blood flow rate, microvascular resistance, and coronary flow reserve. Q_{CFD} is suitable for use in the catheter laboratory and requires no dedicated catheters, wires or infusions. Q_{CFD} measures blood flow and microvascular resistance in absolute units and allows microvascular and epicardial disease to be differentiated, quantified and separately assessed, with the potential to improve diagnostic accuracy and clinical management.